Korean J Physiol Pharmacol 2016;20(3):269-277
http://dx.doi.org/10.4196/kjpp.2016.20.3.269

KJPP

Original Article

Ellagic acid plays a protective role against UV-B-induced oxidative stress by up-regulating antioxidant components in human dermal fibroblasts

Beomyeol Baek[1,#], Su Hee Lee[2,#], Kyunghoon Kim[2,*], Hye-Won Lim[3], and Chang-Jin Lim[1,*]

[1]*Department of Biochemistry and* [2]*Department of Biological Sciences, College of Natural Sciences, Kangwon National University, Chuncheon 24341,* [3]*Shebah Biotech Inc., Chuncheon 24398, Korea*

ARTICLE INFO

Received December 2, 2015
Revised February 26, 2016
Accepted March 15, 2016

***Correspondence**
Kyunghoon Kim
E-mail: kkim@kangwon.ac.kr
Chang-Jin Lim
E-mail: cjlim@kangwon.ac.kr

Key Words
Ellagic acid
Glutathione
Superoxide dismutase
UV-B radiation

[#]These authors contributed equally to this work.

ABSTRACT Ellagic acid (EA), an antioxidant polyphenolic constituent of plant origin, has been reported to possess diverse pharmacological properties, including anti-inflammatory, anti-tumor and immunomodulatory activities. This work aimed to clarify the skin anti-photoaging properties of EA in human dermal fibroblasts. The skin anti-photoaging activity was evaluated by analyzing the reactive oxygen species (ROS), matrix metalloproteinase-2 (MMP-2), total glutathione (GSH) and superoxide dismutase (SOD) activity levels as well as cell viability in dermal fibroblasts under UV-B irradiation. When fibroblasts were exposed to EA prior to UV-B irradiation, EA suppressed UV-B-induced ROS and proMMP-2 elevation. However, EA restored total GSH and SOD activity levels diminished in fibroblasts under UV-B irradiation. EA had an up-regulating activity on the UV-B-reduced Nrf2 levels in fibroblasts. EA, at the concentrations used, was unable to interfere with cell viabilities in both non-irradiated and irradiated fibroblasts. In human dermal fibroblasts, EA plays a defensive role against UV-B-induced oxidative stress possibly through an Nrf2-dependent pathway, indicating that this compound has potential skin anti-photoaging properties.

INTRODUCTION

Ellagic acid (EA; 2,3,7,8-tetrahydroxy-chromeno[5,4,3-cde]-chromene-5,10-dione, Fig. 1) is a fused four-ring polyphenolic compound that is present in numerous vegetables and fruits, including green tea, pomegranate, strawberries, blackberries, raspberries, nuts, grapes and others [1]. EA is abundant as ellagitannins and is released from ellagitannins by the gut microflora [2]. EA has a wide array of physiological functions, including antioxidant, antiviral, antibacterial, anti-inflammatory, anticarcinogenic, antifibrotic, antiplasmodial and chemopreventive activities [3-5]. Most of its currently known pharmacological properties are based, at least partly, upon its antioxidant activity.

The antioxidant properties of EA have been extensively verified using a variety of *in vitro* and *in vivo* methodologies. Its

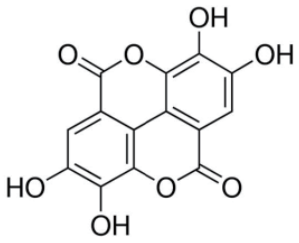

Fig. 1. The chemical structure of ellagic acid (EA).

Author contributions: B.B. and S.H.L. performed the experiment and analyzed the data. H.W.L. supervised and coordinated the experiment. K.K. and C.J.L. designed the research and wrote the manuscript.

antioxidant capability was proposed to be primarily mediated by the four hydroxyl groups present in its structure that scavenge both hydroxyl and superoxide anion radicals [6]. EA stimulates 2,2-diphenyl-1-picrylhydrazyl radical scavenging, superoxide dismutase (SOD), catalase and glutathione peroxidase activities; however, EA inhibits lipid peroxidation in the Chinese hamster lung cell line V79-4 [7]. *In vitro* radical scavenging and antioxidant capacities of EA were further confirmed using various analytical methods, which can measure hydroperoxide, 2,2'-azino-bis(3-ethylbenzthiazoline-6-sulfonic acid) radical and superoxide anion radical scavenging activities, total antioxidant activity by ferric thiocyanate, ferrous ion-chelating activity and ferric ion-reducing ability [8]. In an aqueous solution at physiological pH, EA, in the form of an anion, deactivates a wide variety of free radicals generated in biological systems, and EA anions are continuously regenerated after scavenging two free radicals per cycle [1]. Regeneration of an EA anion gives rise to an advantageous and unusual compound that enhances EA antioxidant activity at low concentrations [1]. EA metabolites also efficiently scavenge a wide variety of free radicals [1].

UV radiation, especially UV-B (280~315 nm) radiation, causes skin photoaging, which is defined as premature aging due to repeated exposure to the radiation and results from a photo-oxidation reaction that disrupts the antioxidant status of skin cells and increases the cellular reactive oxygen species (ROS) levels [9-12]. Enhanced ROS levels induce the production of matrix metalloproteinases (MMPs), a large and complex family of zinc-dependent endopeptidases capable of degrading essentially all components of the extracellular matrix, and lead to skin damage, subsequently causing skin photoaging [13,14]. Collagen degradation is associated with MMP induction, and MMPs are secreted from epidermal keratinocytes and dermal fibroblasts [15]. Skin photoaging under oxidative stress is closely linked with dermal extracellular matrix deterioration due to increased MMP expression and decreased collagen synthesis [16,17]. Limited findings on the beneficial effects of EA in skin cells under UV irradiation have been reported. EA suppresses UV-A-induced ROS generation, malondialdehyde formation, DNA damage and apoptosis but enhances heme oxygenase-1 and SOD expression [18]. EA prevents the UV-B-induced inflammatory cascade by reducing proinflammatory mediators such as interleukin (IL)-1β, IL-6, IL-8 and tumor necrosis factor-α and enhancing IL-10 with an anti-inflammatory function in keratinocytes [19].

In the present work, the skin anti-photoaging properties of EA were clarified by evaluating ROS and MMP-2 levels as well as antioxidant-related components, including total glutathione (GSH), SOD and Nrf2, as a master regulator of antioxidant systems, in human dermal fibroblasts under UV-B irradiation.

METHODS

Materials and chemicals

Ellagic acid (EA, purity≥95%), gelatin, Bradford reagent, 3-(4,5-dimethylthiazol-2-yl)-2,5-diphenyltetrazolium bromide (MTT), 2',7'-dichlorodihydrofluorescein diacetate (DCFH-DA), dihydrorhodamine 123, 5,5'-dithiobis(2-nitrobenzoic acid) (DTNB), glutathione reductase (GR), reduced glutathione (GSH), NADPH, cytochrome c, catalase, xanthine, and xanthine oxidase were obtained from Sigma-Aldrich Chemical Co. (St Louis, MO, USA). Fetal bovine serum (FBS), Dulbecco's modified Eagle's medium (DMEM) and penicillin-streptomycin were purchased from HyClone Laboratories Inc. (Logan, UT, USA). Cell lysis buffer was obtained from Promega Korea (Seoul, Korea). All other chemicals used were of the highest grade commercially available.

Cell culture

The human dermal fibroblast cell line CCD986sk (ATCC, Manassas, VA, USA) was grown in DMEM containing 10% heat-inactivated FBS, 100 U/ml penicillin and 100 μg/ml streptomycin in a humidified atmosphere with 5% CO_2 at 37°C. Prior to the treatment, 1×10^5 mammalian cells, seeded on 24-well plates, were cultured overnight, washed twice with 1 ml phosphate-buffered saline (PBS), and then incubated with 1 ml FBS-free medium. Following UV-B irradiation and/or EA treatment, the cells were grown under the same culture conditions described above.

UV-B irradiation

As an artificial UV-B source, an ultraviolet lamp (peak, 312 nm; model VL-6M, Vilber Lourmat, Marine, France) was used. A radiometer (model VLX-3W, Vilber Lourmat, Marine, France) with a sensor (bandwidth, 280 to 320 nm; model CX-312, Vilber Lourmat, Marine, France) was used to monitor radiation intensity. Fibroblasts were irradiated at 25°C with UV-B radiation at 70 mJ/cm^2.

Preparation of cellular lysate

Adherent cells were washed twice with PBS and stored on ice for 5 min. The cells were scraped off the bottom of a dish with a cell scraper and centrifuged at 15,000 rpm for 10 min. The cell pellets were resuspended in cell lysis buffer [25 mmol/L Tris-phophate (pH 7.8), 2 mmol/L 1,2-diaminocyclohexane-N,N,Nv,Nv-tetraactic acid, 2 mmol/L dithiothreitol, 10% glycerol, 1% Triton X-100] and stored for 30 min on ice. Cellular lysate was obtained after centrifugation at 15,000 rpm for 15 min. Protein contents in cellular lysates were determined according to the Bradford method [20] using bovine serum albumin as a standard.

Quantitation of intracellular ROS

To fluorometrically determine intracellular ROS levels in cultured fibroblasts, a redox-sensitive fluorescent probe DCFH-DA, which generates fluorescent 2',7'-dichlorofluorescein (DCF; $\lambda_{excitation}$=485 nm, $\lambda_{emission}$=530 nm) upon enzymatic reduction and subsequent oxidation by ROS, was used as previously described [21]. After treatment with EA and/or 20 μmol/L DCFH-DA for 30 min at 37°C, the cells were washed twice with 1 ml FBS-free medium. Next, the cells were resuspended in 1 ml FBS-free medium and irradiated with UV-B radiation. The intracellular ROS levels were immediately quantitated using a Multi-Mode Microplate Reader (Synergy™ Mx, BioTek Instruments, Winooki, VT, USA).

For confocal microscopic analysis [21], the cells were treated with EA and/or 20 μmol/L dihydrorhodamine 123 for 30 min at 37°C, irradiated with UV-B radiation, and immediately analyzed using a Confocal Laser Scanning Microscope (Fluoview-FV300, Olympus, Tokyo, Japan). The assays were repeated at least three times.

Cell viability assay

To determine the cellular survival of fibroblasts in the presence of EA, cell viabilities were determined using an MTT assay, which assesses metabolic activity [22]. The cells were treated with EA for 30 min., and after removing the medium by suction, the cells were treated with 5 μg/ml MTT in medium for 4 h. The cells were then lysed with dimethyl sulfoxide, and the amount of formazan, generated from MTT reduction by the mitochondria of living cells, was determined by measuring the absorbance at a wavelength of 540 nm.

Gelatin zymography

MMP-2 gelatinolytic activity in conditioned medium was determined using zymographic analysis as previously described [23]. The cells were further incubated for 24 h at 37°C and washed twice with 1 ml PBS. The cells in 1 ml FBS-free medium were treated with EA for 30 min and irradiated with UV-B radiation. The conditioned medium, taken from fibroblasts culture incubated for 24 h at 37°C, was fractionated on 10% (w/v) SDS-PAGE gel impregnated with 1 mg/ml gelatin under non-reducing conditions. Proteins in the gel were renatured by shaking with 2.5% Triton X-100 at room temperature for 30 min two times and were then incubated in incubation buffer (50 mmol/L Tris buffer, pH 7.8, 5 mmol/L $CaCl_2$, 0.15 mol/L NaCl, 1% Triton X-100) for 24 h. After the gel was stained with 0.1% Coomassie Brilliant Blue R-250, gelatin-degrading enzyme activities were denoted as clear zones against a blue background. The MMP-2 activity band was identified in accordance with its molecular mass, which was estimated by molecular mass markers.

Western blotting analysis

To detect MMP-2 and Nrf2 proteins in the cellular lysate, western blotting analysis was performed using anti-MMP-2 (ALX-210-753, Enzo Life Sciences, Farmingdale, NY, USA) and ant-Nrf2 (ab31163, Abcam, Cambridge, MA, USA) antibodies as the primary antibodies. The cellular lysates were run on a 10% (w/v) SDS-PAGE and electrotransferred to PVDF membranes. The membranes were blocked with blocking buffer (2% BSA in 1X TBS-Tween 20), probed with primary antibody overnight at 4°C, incubated with secondary antibody (goat anti-rabbit IgG-pAb-HRP-conjugate; ADI-SAB-300, Enzo Life Sciences, Farmingdale, NY, USA) for 1 h at room temperature, and developed using an enhanced West-save up™ (AbFrontier, Seoul, Korea).

Determination of total GSH in cellular lysate

As previously described [24], the total GSH content in the cellular lysate was determined using an enzymatic recycling assay based on GR. The reaction mixture (200 μl), containing 175 mmol/L KH_2PO_4, 6.3 mmol/L EDTA, 0.21 mmol/L NADPH, 0.6 mmol/L DTNB, 0.5 U/ml GR and cellular lysate, was incubated at 25°C. Absorbance at 412 nm was monitored using a microplate reader. Total GSH content in the cellular lysates was reported as μg/mg protein.

Determination of total SOD activity

As previously described [25], the total SOD activity in cellular lysate was spectrophotometrically determined as reduced cytochrome c with the xanthine/xanthine oxidase system. The reaction mixture (200 μl) contained 50 mmol/L phosphate buffer (pH 7.4), 0.01 U/ml xanthine oxidase, 0.1 mmol/L EDTA, 1 μmol/L catalase, 0.05 mmol/L xanthine, 20 μmol/L cytochrome c and cellular lysate. A change in absorbance was monitored at 550 nm.

Statistical analysis

The results are shown as the mean±SD. Comparisons between experimental groups were statistically analyzed using unpaired Student's *t*-test. A p-value of less than 0.05 was considered statistically significant.

RESULTS

Down-regulation of UV-B-induced ROS elevation

The fibroblasts were exposed to varying concentrations (0, 5, 12 or 30 μmol/L) of EA prior to irradiation with 70 mJ/cm^2 UV-B radiation. As shown in Fig. 2A, the UV-B irradiation alone, in the absence of EA treatment, caused an approximately 11.5-fold

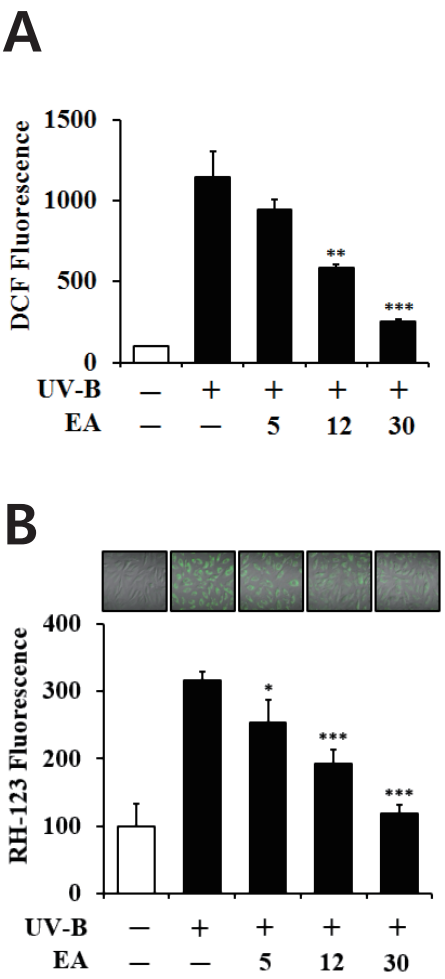

Fig. 2. Attenuating effect of EA on the reactive oxygen species (ROS) elevation in human dermal fibroblasts under UV-B irradiation. Fibroblasts were subjected to fresh media with the varying concentrations (0, 5, 12 or 30 μmol/L) of EA for 30 min before irradiation. The intracellular ROS levels were determined using both DCFH-DA in a microplate fluorometer (A) and dihydrorhodamine 123 via confocal microscopic analysis (B). In A, ROS levels are represented as DCF fluorescence arbitrary units expressed as the percentage of control. In the lower panel of B, the ROS-associated fluorescent signals were quantified using Adobe Photoshop software. Data are presented as % of control versus the non-irradiated control (Mean±SD, n=3). *p<0.05; **p<0.01; ***p<0.001 versus the non-treated control (UV-B irradiation alone).

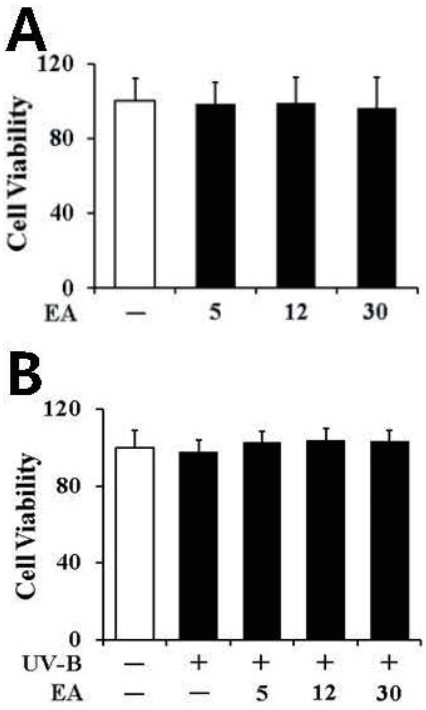

Fig. 3. Non-toxic effects of EA on the cellular viability in human dermal fibroblasts without (A) or with (B) UV-B irradiation. Fibroblasts were subjected to fresh media with the varying concentrations (0, 5, 12 or 30 μmol/L) of EA for 30 min before irradiation. The viable cell numbers were determined using MTT assay. Data are presented as % of control versus the non-treated (A) or non-irradiated (B) control (Mean±SD, n=3).

enhancement in the ROS level compared with the non-irradiated control cells. EA attenuated UV-B-induced ROS elevation in a concentration-dependent fashion (Fig. 2A). EA treatment at 5, 12 and 30 μmol/L reduced the UV-B-induced ROS enhancement to 82.1%, 51.1% and 22.3%, respectively, of the ROS levels induced by UV-B irradiation alone (Fig. 2A). The IC_{50} value of EA was estimated to be 12.2 μmol/L. As shown in Fig. 2B, this attenuating effect of EA was also confirmed using confocal microscopic analysis, which showed that UV-B irradiation alone, in the absence of EA treatment, produced an approximately 3.2-fold elevation in the ROS level, compared with the non-irradiated control cells (Fig. 2B). EA treatment at 5, 12 and 30 μmol/L diminished the UV-B-induced ROS enhancement to 80.0%, 60.0% and 37.0% of the levels induced by UV-B irradiation alone, respectively (Fig. 2B). Overall, EA down-regulates UV-B-induced ROS elevation in human dermal fibroblasts.

No cytotoxicity

To detect whether EA at the applied concentrations is cytotoxic to cultured fibroblasts, its effects on the cellular viabilities of fibroblasts were determined using an MTT assay. As shown in Fig. 3A, in the absence of UV-B irradiation, 5, 12 and 30 μmol/L EA exhibited no modulatory effect on fibroblast cellular viability. UV-B irradiation alone, in the absence of EA treatment, did not change fibroblast cellular viability, and the viabilities remained similar to the viability of non-irradiated fibroblasts (Fig. 3B). As shown in Fig. 3B, EA did not alter fibroblast viabilities under UV-B irradiation (Fig. 3B). Overall, at the applied concentrations, EA did not exhibit any cytotoxic effects on cultured fibroblasts, irrespective of UV-B irradiation.

Attenuation of UV-B-induced MMP-2 elevation

UV radiation enhances the production of certain MMP family

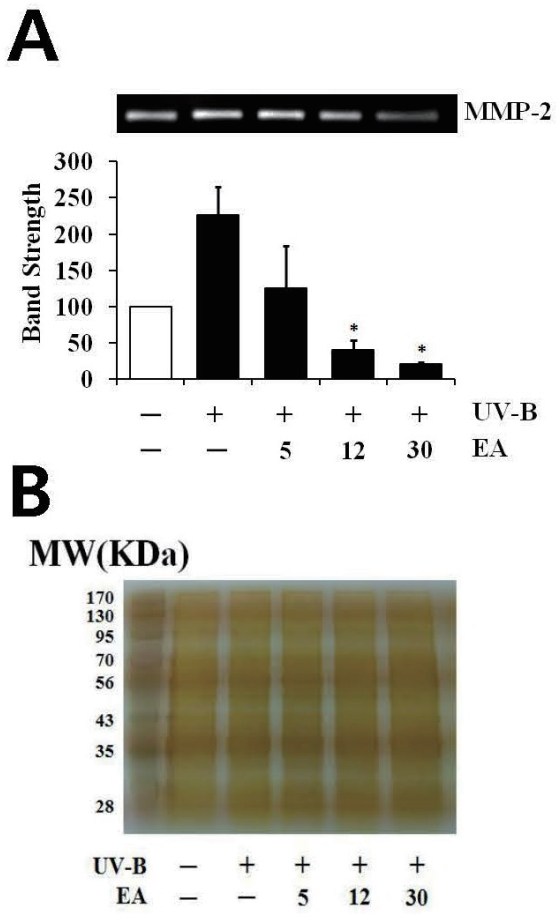

Fig. 4. Attenuating effect of EA on the gelatinolytic activity of promatrix metalloproteinase-2 (proMMP-2) in the conditioned media from human dermal fibroblasts under UV-B irradiation. Fibroblasts were subjected to fresh media with the varying concentrations (0, 5, 12 or 30 μmol/L) of EA for 30 min before irradiation. In A, the proMMP-2 gelatinolytic activity in conditioned medium was detected using gelatin zymography. The relative band strength was determined with densitometry using ImageJ software. In B, the equal loading of conditioned media was shown by the silver staining. Data are presented as % of control versus the non-irradiated control (Mean±SD, n=3). *p<0.05 versus the non-treated control (UV-B irradiation alone).

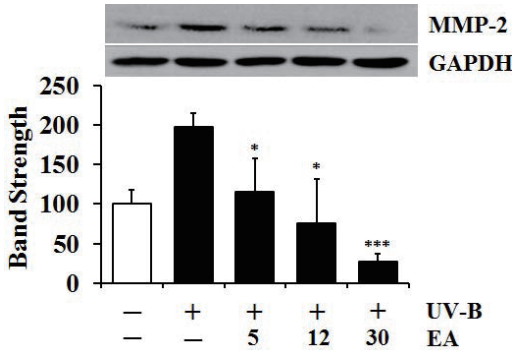

Fig. 5. Attenuating effect of EA on promatrix metalloproteinase-2 (proMMP-2) protein levels in human dermal fibroblasts under UV-B irradiation. Fibroblasts were subjected to fresh media with the varying concentrations (0, 5, 12 or 30 μmol/L) of EA for 30 min before the irradiation. The proMMP-2 proteins were determined using western blotting analysis with anti-MMP-2 antibodies. GAPDH was used as a protein loading control. The relative band strength was determined with densitometry using ImageJ software. Data are presented as % of control versus the non-irradiated control (Mean±SD, n=3). *p<0.05; ***p<0.001 versus the non-treated control (UV-B irradiation alone).

members; therefore, chronic exposure to UV radiation impairs the normal architecture of the skin, subsequently leading to skin photoaging [26]. UV-B irradiation alone significantly enhanced proMMP-2 gelatinolytic activity in fibroblasts and EA attenuated the UV-B-induced proMMP-2 gelatinolytic activity in fibroblasts in a concentration-dependent fashion (Fig. 4A). As shown in Fig. 4B, silver staining was used to prove the equal loading of conditioned media. EA diminished UV-B-induced elevation in proMMP-2 gelatinolytic activity; therefore, proMMP-2 protein levels in fibroblast cellular lysates were examined using western blotting analysis. Expectedly, UV-B irradiation alone markedly enhanced the proMMP-2 protein levels (Fig. 5). EA at 5, 12 and 30 μmol/L was able to attenuate the UV-B-induced proMMP-2 protein levels in cellular lysates in a concentration-dependent fashion (Fig. 5). Collectively, EA down-regulates UV-B-induced proMMP-2 gelatinolytic activity by attenuating proMMP-2 protein production in dermal fibroblasts.

EA restores UV-B-attenuated total GSH levels

Consistent with a previous finding [27], the total GSH content was significantly decreased in fibroblasts irradiated with UV-B radiation (Fig. 6A). Prior treatment with 5, 12, and 30 μmol/L EA increased the UV-B-diminished total GSH levels by 1.7-, 2.6- and 3.1-fold, respectively, compared with the irradiated fibroblasts that did not receive EA treatment (Fig. 6A). Taken together, this finding suggests that the GSH-enhancing effects of EA combat the deleterious effects of UV-B irradiation.

Up-regulation of total SOD activity

As shown in Fig. 6B, total SOD activity was significantly diminished by irradiation with UV-B radiation in dermal fibroblasts; however, this reduction was restored by treatment with EA. In total, 5, 12 and 30 μmol/L EA increased the SOD activities by 2.0-, 2.5- and 3.2-fold, respectively, compared with the UV-B-irradiated fibroblasts not treated with EA (Fig. 6B). Taken together, in dermal fibroblasts, EA up-regulates SOD activity that was decreased under UV-B irradiation.

Enhancement of Nrf2 levels

The Nrf2 levels in the UV-B-irradiated cells were dropped to 74.3% of that of the non-irradiated control (Fig. 7). EA at 5, 12 and

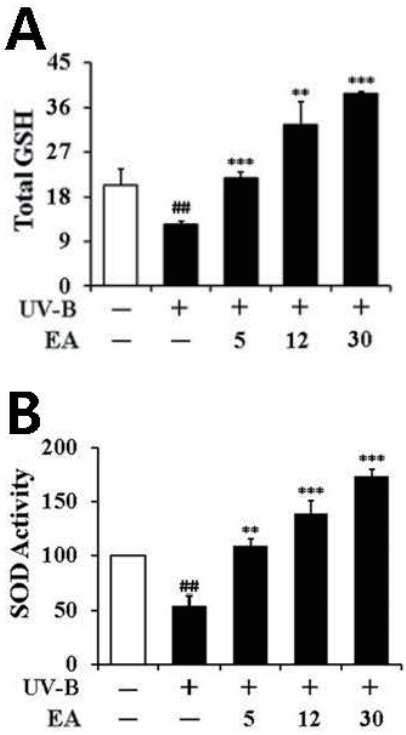

Fig. 6. Enhancing effects of EA on the total GSH (A) and SOD (B) activity levels in human dermal fibroblasts under UV-B irradiation. Fibroblasts were subjected to fresh media with the varying concentrations (0, 5, 12 or 30 μmol/L) of EA for 30 min before the irradiation. In A, total GSH content, expressed as μg/mg protein, was determined with an enzymatic recycling assay using GR. In B, total SOD activity was measured using a spectrophotometric assay and presented as % of control versus the non-irradiated control (Mean±SD, n=3). ##p<0.01 versus non-irradiated control; **p<0.01; ***p<0.001 versus non-treated control (UV-B irradiation alone).

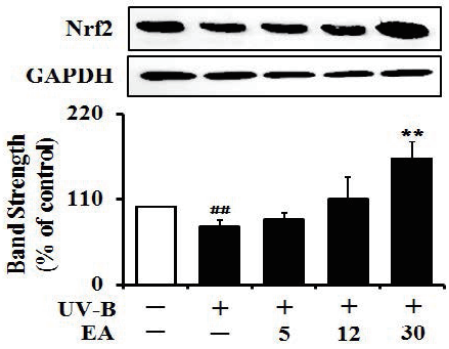

Fig. 7. Enhancing effect of EA on the Nrf2 levels in human dermal fibroblasts under UV-B irradiation. Fibroblasts were subjected to fresh media with the varying concentrations (0, 5, 12 or 30 μmol/L) of EA for 30 min before the irradiation. The Nrf2 proteins were determined using western blotting analysis with anti-Nrf2 antibodies. GAPDH was used as a protein loading control. The relative band strength was determined with densitometry using ImageJ software. Data are presented as % of control versus the non-irradiated control (Mean±SD, n=3). ##p<0.01 versus non-irradiated control; **p<0.01 versus non-treated control (UV-B irradiation alone).

30 μmol/L could cause an enhancement in the UV-B-reduced Nrf2 levels by 1.1-, 1.5- and 2.2-fold, respectively, compared with that of the irradiation only (Fig. 7). Collectively, EA has an up-regulating effect on the UV-B-reduced Nrf2 levels in human dermal fibroblasts.

DISCUSSION

EA, a polyphenolic phytonutrient occurring naturally in various plant foods, including berries, nuts and vegetables, is known to possess an extensive array of biologically valuable properties [28]. EA has shown potent *in vitro* and *in vivo* antioxidant activity in diverse experimental models; therefore, EA has received much attention recently. Various biological activities of EA mediated by its antioxidant activity have already been elucidated using different experimental systems. EA have been documented to exhibit protective properties by suppressing oxidative stress-related biochemical markers and/or by enhancing antioxidant-related biochemical markers in oxidative stress-induced hepatocytes [29], hyperlipidemic rabbits [30], oxidative-damaged brains and sciatic nerves in diabetic rats [31], cyclophosphamide-treated rat spermatogenic cells [32], isoproterenol-treated male rats during myocardial infarction [33], and human lung carcinoma cells [34]. EA displays anti-inflammatory effects against carrageenan-induced inflammation in rats through the reduction of nitric oxide, malondialdehyde, interleukin-1β, tumor necrosis factor-α, cyclooxygenase-2 and nuclear factor-κB expression and the induction of GSH and interleukin-10 production [35]. Nevertheless, the strong antioxidant activity of EA still deserves further investigation, and few studies have investigated the beneficial effects of EA on human skin tissue. Furthermore, the advantageous effects of EA on skin oxidative damage have not yet been clearly elucidated.

The present work was designed to clarify the skin anti-photoaging activities of EA. Specifically, UV-B radiation at 70 mJ/cm^2, the intensity chosen from a preliminary test, caused a marked increase in the intracellular ROS levels of cultured fibroblasts. This result confirms the establishment of UV-B-induced oxidative stress status in cultured fibroblasts, which mimics the triggering stage of human skin cells chronically exposed to UV-B radiation from sunlight. EA attenuates the intracellular ROS levels in cultured fibroblasts under UV-B-induced oxidative stress in a concentration-dependent manner.

Elevated intracellular ROS levels in skin cells under UV-B-induced oxidative stress are thought to initiate skin photoaging by sequentially increasing several types of MMP activities.

Based on previous findings, enhanced ROS levels due to UV radiation induce the production and secretion of MMPs, including MMP-1, MMP-2, MMP-3, MMP-9 and/or MMP-13, in the epidermis and dermis, which contribute to skin damage

and photoaging [36,37]. Skin photoaging is initiated by increased intracellular ROS levels and/or MMP activities; therefore, the obstruction of their elevation has been hypothesized to be a powerful strategy to prevent or attenuate skin photoaging. Several natural extracts and natural constituents have already been shown to possess blocking activities in skin cells. For example, *Labisia pumila* aqueous extract restores UV-B-suppressed collagen synthesis of human fibroblasts to normal levels and down-regulates UV-B-induced MMP-9 expression in keratinocytes [38]. *Gynura procumbens* ethanol extract diminishes UV-B-induced MMP-1 expression, MMP-9 activity, and ROS production in human primary dermal fibroblasts [39]. Sargachromenol, a plastoquinone purified from *Sargassum horneri*, down-regulates UV-B-induced MMP-2 mRNA levels in dermal fibroblasts [40]. In the present work, we demonstrate that EA reduces MMP-2 activity and production significantly enhanced by the increased intracellular ROS levels in cultured fibroblasts under UV-B-induced oxidative stress. This EA blocking activity on MMP-2 elevation may result from its ROS-scavenging activity, which requires further verification. MMP-2 down-regulation by EA is partially consistent with the suppressive effect of EA on MMP-2 secretion from human vascular endothelial cells [41].

GSH in living cells plays essential roles in maintaining cellular redox homeostasis and protecting against oxidative stress and injury. UV-B radiation-induced GSH depletion in cultured human fibroblasts mimics the pathogenesis of several cutaneous disorders, which is possibly implicated in the decreased activity of γ-glutamylcysteine synthetase and diminished cysteine uptake through the functional inhibition of a cysteine transporter on the cell membrane [27]. Inactivation of the cysteine transporter system is proven to be a major contributor to the UV-B-induced reduction of GSH levels in human epidermal keratinocytes [27]. When mouse lenses were exposed to UV-B radiation, simultaneous attenuation in ATP and GSH were observed; however, their attenuation was prevented by caffeine [42]. In the aquatic worm tubifex, UV-B radiation induces the production of singlet oxygen, superoxide anions, and hydroxyl radicals, but diminishes GSH, DNA, RNA, and protein levels [43]. In the present work, UV-B irradiation markedly attenuated the total GSH levels in cultured dermal fibroblasts, which is similar to the findings observed with other types of cells. EA treatment prior to UV-B irradiation increased UV-B-attenuated GSH levels in a concentration-dependent manner in cultured fibroblasts. EA at the concentrations of 12 and 30 μM increased the total GSH levels above the levels in non-irradiated cells via a currently unknown mechanism.

Here, this work suggests that EA restores GSH and SOD depletion caused by UV-B radiation exposure. Although the mechanisms of these restoring activities remain unknown, restoration of antioxidant components such as GSH and SOD may trigger an event that leads to the attenuation of ROS enhancement in dermal fibroblasts. This finding suggests a possibility that the skin anti-photoaging activities of EA are based on the activation or induction of antioxidant components that play a role in ROS attenuation. Nrf2 (nuclear factor-E2-related factor 2) was previously suggested to play a crucial role in the protection against UV-B-induced photoaging, based upon the fact that UV-B-irradiated *nrf2*$^{-/-}$ mice exhibited accelerated photoaging symptoms and decreased cutaneous GSH level [44]. Nrf2 plays a protective role against UV-induced apoptosis *in vitro* and acute sunburn reactions *in vivo*, and prevents photoaging by maintaining high levels of antioxidants, such as GSH, in the skin [45]. Dietary EA also plays a protective role against oxidant-induced endothelial dysfunction and atherosclerosis partly via Nrf2 activation in mice [46]. This work demonstrates that EA has an up-regulating activity on the UV-B-reduced Nrf2 levels in fibroblasts, implying that its defensive properties against photooxidative stress occur via the mediation of Nrf2. In a similar way, the antioxidant potential of EA is correlated with the increased expression of heme oxygenase-1 and SOD in human keratinocyte cells, which is followed by the down-regulation of Keap1 and the augmented nuclear translocation and transcriptional activation of Nrf2 with or without UV-A irradiation [47]. Systemic administration of the apocarotenoid bixin, a natural food additive consumed worldwide, was also found to protect skin against solar UV-induced damage through activation of Nrf2 [48].

In conclusion, the potential skin anti-photoaging activity of EA was clarified in dermal fibroblasts cells exposed to UV-B radiation. EA suppresses the UV-B-induced intracellular ROS levels and proMMP-2 production and secretion and enhances UV-B-depleted total GSH levels and SOD activity. EA may elicit its skin anti-photoaging property through the down-regulation of UV-B-induced MMP-2 via an ROS-dependent mechanism, which results from the restoration of total GSH and SOD activity depleted under UV-B irradiation. EA also has an up-regulating activity on the UV-B-reduced Nrf2 levels, suggesting that its defensive properties are based upon the mediation of Nrf2. However, elucidation of precise mechanism(s) on these effects of EA will require further experimental approaches. EA is a plausible candidate used as a natural resource for manufacturing anti-photoaging cosmetics, which may have similar or enhanced activities with fewer side effects.

ACKNOWLEDGEMENTS

This study was supported by a grant of the Korean Health Technology R&D Project, Ministry of Health & Welfare, Republic of Korea (Grant No. HN12C0060).

CONFLICTS OF INTEREST

The authors declare no conflicts of interest.

REFERENCES

1. Galano A, Francisco Marquez M, Pérez-González A. Ellagic acid: an unusually versatile protector against oxidative stress. *Chem Res Toxicol*. 2014;27:904-918.
2. Larrosa M, Tomás-Barberán FA, Espín JC. The dietary hydrolysable tannin punicalagin releases ellagic acid that induces apoptosis in human colon adenocarcinoma Caco-2 cells by using the mitochondrial pathway. *J Nutr Biochem*. 2006;17:611-625.
3. Goodwin EC, Atwood WJ, DiMaio D. High-throughput cell-based screen for chemicals that inhibit infection by simian virus 40 and human polyomaviruses. *J Virol*. 2009;83:5630-5639.
4. Rogerio AP, Fontanari C, Borducchi E, Keller AC, Russo M, Soares EG, Albuquerque DA, Faccioli LH. Anti-inflammatory effects of Lafoensia pacari and ellagic acid in a murine model of asthma. *Eur J Pharmacol*. 2008;580:262-270.
5. Seeram NP, Adams LS, Henning SM, Niu Y, Zhang Y, Nair MG, Heber D. In vitro antiproliferative, apoptotic and antioxidant activities of punicalagin, ellagic acid and a total pomegranate tannin extract are enhanced in combination with other polyphenols as found in pomegranate juice. *J Nutr Biochem*. 2005;16:360-367.
6. Pari L, Sivasankari R. Effect of ellagic acid on cyclosporine A-induced oxidative damage in the liver of rats. *Fundam Clin Pharmacol*. 2008;22:395-401.
7. Han DH, Lee MJ, Kim JH. Antioxidant and apoptosis-inducing activities of ellagic acid. *Anticancer Res*. 2006;26:3601-3606.
8. Kilic I, Yeşiloğlu Y, Bayrak Y. Spectroscopic studies on the antioxidant activity of ellagic acid. *Spectrochim Acta A Mol Biomol Spectrosc*. 2014;130:447-452.
9. Birch-Machin MA, Swalwell H. How mitochondria record the effects of UV exposure and oxidative stress using human skin as a model tissue. *Mutagenesis*. 2010;25:101-107.
10. Barresi C, Stremnitzer C, Mlitz V, Kezic S, Kammeyer A, Ghannadan M, Posa-Markaryan K, Selden C, Tschachler E, Eckhart L. Increased sensitivity of histidinemic mice to UVB radiation suggests a crucial role of endogenous urocanic acid in photoprotection. *J Invest Dermatol*. 2011;131:188-194.
11. Ikehata H, Ono T. The mechanisms of UV mutagenesis. *J Radiat Res*. 2011;52:115-125.
12. Peres PS, Terra VA, Guarnier FA, Cecchini R, Cecchini AL. Photoaging and chronological aging profile: Understanding oxidation of the skin. *J Photochem Photobiol B*. 2011;103:93-97.
13. Curran S, Murray GI. Matrix metalloproteinases in tumour invasion and metastasis. *J Pathol*. 1999;189:300-308.
14. Pygmalion MJ, Ruiz L, Popovic E, Gizard J, Portes P, Marat X, Lucet-Levannier K, Muller B, Galey JB. Skin cell protection against UVA by Sideroxyl, a new antioxidant complementary to sunscreens. *Free Radic Biol Med*. 2010;49:1629-1637.
15. Lee YM, Kim YK, Kim KH, Park SJ, Kim SJ, Chung JH. A novel role for the TRPV1 channel in UV-induced matrix metalloproteinase (MMP)-1 expression in HaCaT cells. *J Cell Physiol*. 2009;219:766-775.
16. Chae S, Piao MJ, Kang KA, Zhang R, Kim KC, Youn UJ, Nam KW, Lee JH, Hyun JW. Inhibition of matrix metalloproteinase-1 induced by oxidative stress in human keratinocytes by mangiferin isolated from Anemarrhena asphodeloides. *Biosci Biotechnol Biochem*. 2011;75:2321-2325.
17. Kim MS, Oh GH, Kim MJ, Hwang JK. Fucosterol inhibits matrix metalloproteinase expression and promotes type-1 procollagen production in UVB-induced HaCaT cells. *Photochem Photobiol*. 2013;89:911-918.
18. Hseu YC, Chou CW, Senthil Kumar KJ, Fu KT, Wang HM, Hsu LS, Kuo YH, Wu CR, Chen SC, Yang HL. Ellagic acid protects human keratinocyte (HaCaT) cells against UVA-induced oxidative stress and apoptosis through the upregulation of the HO-1 and Nrf-2 antioxidant genes. *Food Chem Toxicol*. 2012;50:1245-1255.
19. Lembo S, Balato A, Di Caprio R, Cirillo T, Giannini V, Gasparri F, Monfrecola G. The modulatory effect of ellagic acid and rosmarinic acid on ultraviolet-B-induced cytokine/chemokine gene expression in skin keratinocyte (HaCaT) cells. *Biomed Res Int*. 2014. doi: 10.1155/2014/346793.
20. Bradford MM. A rapid and sensitive method for the quantitation of microgram quantities of protein utilizing the principle of protein-dye binding. *Anal Biochem*. 1976;72:248-254.
21. Royall JA, Ischiropoulos H. Evaluation of 2',7'-dichlorofluorescin and dihydrorhodamine 123 as fluorescent probes for intracellular H2O2 in cultured endothelial cells. *Arch Biochem Biophys*. 1993;302:348-355.
22. Freshney RI. Culture of animal cells: a manual of basic technique. 3rd ed. New York: Wiley-Liss Press; 1994.
23. Kleiner DE, Stetler-Stevenson WG. Quantitative zymography: detection of picogram quantities of gelatinases. *Anal Biochem*. 1994;218:325-329.
24. Nakagawa K, Saijo N, Tsuchida S, Sakai M, Tsunokawa Y, Yokota J, Muramatsu M, Sato K, Terada M, Tew KD. Glutathione-S-transferase pi as a determinant of drug resistance in transfectant cell lines. *J Biol Chem*. 1990;265:4296-4301.
25. Lee YY, Kim HG, Jung HI, Shin YH, Hong SM, Park EH, Sa JH, Lim CJ. Activities of antioxidant and redox enzymes in human normal hepatic and hepatoma cell lines. *Mol Cells*. 2002;14:305-311.
26. Quan T, Qin Z, Xia W, Shao Y, Voorhees JJ, Fisher GJ. Matrix-degrading metalloproteinases in photoaging. *J Investig Dermatol Symp Proc*. 2009;14:20-24.
27. Zhu M, Bowden GT. Molecular mechanism(s) for UV-B irradiation-induced glutathione depletion in cultured human keratinocytes. *Photochem Photobiol*. 2004;80:191-196.
28. Priyadarsini KI, Khopde SM, Kumar SS, Mohan H. Free radical studies of ellagic acid, a natural phenolic antioxidant. *J Agric Food Chem*. 2002;50:2200-2206.
29. Hwang JM, Cho JS, Kim TH, Lee YI. Ellagic acid protects hepatocytes from damage by inhibiting mitochondrial production of reactive oxygen species. *Biomed Pharmacother*. 2010;64:264-270.
30. Yu YM, Chang WC, Wu CH, Chiang SY. Reduction of oxidative stress and apoptosis in hyperlipidemic rabbits by ellagic acid. *J Nutr Biochem*. 2005;16:675-681.
31. Uzar E, Alp H, Cevik MU, Fırat U, Evliyaoglu O, Tufek A, Altun Y. Ellagic acid attenuates oxidative stress on brain and sciatic nerve and improves histopathology of brain in streptozotocin-induced diabetic rats. *Neurol Sci*. 2012;33:567-574.

32. Türk G, Ceribaşi AO, Sakin F, Sönmez M, Ateşşahin A. Antiperoxidative and anti-apoptotic effects of lycopene and ellagic acid on cyclophosphamide-induced testicular lipid peroxidation and apoptosis. *Reprod Fertil Dev*. 2010;22:587-596.
33. Kannan MM, Quine SD. Ellagic acid ameliorates isoproterenol induced oxidative stress: Evidence from electrocardiological, biochemical and histological study. *Eur J Pharmacol*. 2011;659:45-52.
34. Kim YS, Zerin T, Song HY. Antioxidant action of ellagic acid ameliorates paraquat-induced A549 cytotoxicity. *Biol Pharm Bull*. 2013;36:609-615.
35. El-Shitany NA, El-Bastawissy EA, El-desoky K. Ellagic acid protects against carrageenan-induced acute inflammation through inhibition of nuclear factor kappa B, inducible cyclooxygenase and proinflammatory cytokines and enhancement of interleukin-10 via an antioxidant mechanism. *Int Immunopharmacol*. 2014;19:290-299.
36. Fisher GJ, Wang ZQ, Datta SC, Varani J, Kang S, Voorhees JJ. Pathophysiology of premature skin aging induced by ultraviolet light. *N Engl J Med*. 1997;337:1419-1428.
37. Lee YM, Kang SM, Lee SR, Kong KH, Lee JY, Kim EJ, Chung JH. Inhibitory effects of TRPV1 blocker on UV-induced responses in the hairless mice. *Arch Dermatol Res*. 2011;303:727-736.
38. Choi HK, Kim DH, Kim JW, Ngadiran S, Sarmidi MR, Park CS. Labisia pumila extract protects skin cells from photoaging caused by UVB irradiation. *J Biosci Bioeng*. 2010;109:291-296.
39. Kim J, Lee CW, Kim EK, Lee SJ, Park NH, Kim HS, Kim HK, Char K, Jang YP, Kim JW. Inhibition effect of Gynura procumbens extract on UV-B-induced matrix-metalloproteinase expression in human dermal fibroblasts. *J Ethnopharmacol*. 2011;137:427-433.
40. Kim JA, Ahn BN, Kong CS, Kim SK. Protective effect of chromene isolated from Sargassum horneri against UV-A-induced damage in skin dermal fibroblasts. *Exp Dermatol*. 2012;21:630-631.
41. Huang ST, Wang CY, Yang RC, Wu HT, Yang SH, Cheng YC, Pang JH. Ellagic acid, the active compound of phyllanthus urinaria, exerts in vivo anti-angiogenic effect and inhibits MMP-2 activity. Evid Based Complement Alternat Med. 2011. doi: 10.1093/ecam/nep207.
42. Varma SD, Hegde KR, Kovtun S. UV-B-induced damage to the lens in vitro: prevention by caffeine. *J Ocul Pharmacol Ther*. 2008;24:439-444.
43. Misra RB, Babu GS, Ray RS, Hans RK. Tubifex: a sensitive model for UV-B-induced phototoxicity. *Ecotoxicol Environ Saf*. 2002;52:288-295.
44. Hirota A, Kawachi Y, Yamamoto M, Koga T, Hamada K, Otsuka F. Acceleration of UVB-induced photoageing in nrf2 gene-deficient mice. *Exp Dermatol*. 2011;20:664-668.
45. Kim M, Park YG, Lee HJ, Lim SJ, Nho CW. Youngiasides A and C Isolated from youngia denticulatum inhibit UVB-induced MMP expression and promote type I procollagen production via repression of MAPK/AP-1/NF-κB and activation of AMPK/Nrf2 in HaCaT cells and human dermal fibroblasts. *J Agric Food Chem*. 2015;63:5428-5438.
46. Ding Y, Zhang B, Zhou K, Chen M, Wang M, Jia Y, Song Y, Li Y, Wen A. Dietary ellagic acid improves oxidant-induced endothelial dysfunction and atherosclerosis: role of Nrf2 activation. *Int J Cardiol*. 2014;175:508-514.
47. Hseu YC, Chou CW, Senthil Kumar KJ, Fu KT, Wang HM, Hsu LS, Kuo YH, Wu CR, Chen SC, Yang HL. Ellagic acid protects human keratinocyte (HaCaT) cells against UVA-induced oxidative stress and apoptosis through the upregulation of the HO-1 and Nrf-2 antioxidant genes. *Food Chem Toxicol*. 2012;50:1245-1255.
48. Tao S, Park SL, de la Vega MR, Zhang DD, Wondrak GT. Systemic administration of the apocarotenoid bixin protects skin against solar UV-induced damage through activation of NRF2. *Free Radic Biol Med*. 2015;89:690-700.